

# Vanadium-loaded carbon-based monoliths for on-board NO reduction: Influence of nature and concentration of the oxidation agent on activity

A. Boyano<sup>a</sup>, M.C. Iritia<sup>a</sup>, I. Malpartida<sup>b</sup>, M.A. Larrubia<sup>b</sup>,  
L.J. Alemany<sup>b</sup>, R. Moliner<sup>a</sup>, M.J. Lázaro<sup>a,\*</sup>

<sup>a</sup> Instituto de Carboquímica, CSIC, c/Miguel Luesma Castán, E-50018 Zaragoza, Spain

<sup>b</sup> Departamento de Ingeniería Química, Facultad de Ciencias, Campus de Teatinos s/n, Universidad de Málaga, E-29071 Málaga, Spain

Available online 1 April 2008

## Abstract

A series of polymeric carbon-coated monoliths oxidized with either concentrated or 2N HNO<sub>3</sub>, H<sub>2</sub>O<sub>2</sub> or H<sub>2</sub>SO<sub>4</sub> and subsequently loaded with 3 wt.% vanadium were prepared. The influence of the different oxidation treatment conditions on the SCR (selective catalytic reduction) catalytic activity, texture and chemical surface properties were studied. Similar pore distribution and pore volumes were observed for the four oxidized samples, indicating that surface modification of carbon supports has been successfully made without disrupting the original textural structures of activated coated monoliths. The surface chemistry created by the oxidation treatments has two effects on the catalytic activity. One of these is that higher surface acidity results in higher NO reduction up to a certain extent. The highest acidities seem to promote a sufficiently strong NH<sub>3</sub> adsorption on the surface such that the lack of efficient desorption decreases the overall NO conversion efficiency. The other effect is that a low surface acidity does not seem to promote vanadium dispersion and fixation, thereby also resulting in decreased NO reduction efficiency.

© 2008 Elsevier B.V. All rights reserved.

**Keywords:** Functionalization; Carbon-based catalysts; SCR-NH<sub>3</sub>

## 1. Introduction

Today, increasingly stringent regulations require advanced treatment of automotive exhaust to protect the quality of the air and the atmosphere. Among the wide range of treatment technologies that are being developed and optimized, selective catalytic reduction (SCR) of NO<sub>x</sub> is one that has garnered significant attention in the past several years. Various catalysts have been studied for the SCR of NO<sub>x</sub> with NH<sub>3</sub> [1,2], but carbon-based catalysts present two important unique advantages: they are active at lower temperatures [3] and exhibit an activity promotion by SO<sub>2</sub> [4]. As a result, in this study these are proposed for on-board SCR.

Carbon materials are becoming more interesting and promising as supports for heterogeneous catalysts because their porosity and surface chemistry can be controlled. At the same time, they exhibit relatively low reactivity. When activated carbon is used as a support for metallic catalysts,

its performance is expected to be strongly influenced by functional groups present on the carbon surface since they influence metal dispersion, resistance to sintering, and the overall catalytic behaviour [5,6]. In order to form surface carbon–oxygen complexes, liquid oxidation treatments are widely used. This method creates oxygen functionalities while producing only minimal changes in the textural properties. Liquid oxidation is an alternative to methods involving oxidizing gases, which require high temperatures. According to the literature, different oxidizing agents can be used in aqueous solution [7,8]. Each oxidizing agent behaves in a different way, eliciting particular transformations that mostly depend on the characteristics of the reacting agent as well as the nature of the activated carbon [9]. Regardless of the oxidizing agent, however, oxidation treatments introduce three types of surface oxygen complexes: acidic, basic, and neutral [9]. Acidic groups correspond to surface oxides (such as carboxyls, phenolic hydroxyls, lactones, and quinone groups) whose fixation on the surface makes it more hydrophilic and acidic, decreasing the pH of their point of zero charge [10]. These changes contribute to the creation of new surface properties that directly impact activity in two primary ways: (i) provision of

\* Corresponding author. Tel.: +34 976733977; fax: +34 976733318.

E-mail address: [mlazaro@icb.csic.es](mailto:mlazaro@icb.csic.es) (M.J. Lázaro).

anchoring sites for metal precursors during catalyst preparation are based on the amount and type of oxygen surface groups and (ii) the newly created centres with acid–base or redox properties can increase or decrease active phase dispersion and, consequently, catalytic activity [11]. Therefore, the identification and evaluation of these surface functional groups has received much attention from the catalysis field, and various techniques such as XPS, TPD, elemental analysis, FTIR, etc. have successfully been applied to their characterization.

This paper examines the effect of oxidation treatment on the physical–chemical properties of supports and the subsequent impregnation with vanadium as the active phase. Oxidation treatments were carried out in the liquid phase using  $\text{HNO}_3$ ,  $\text{H}_2\text{SO}_4$ , or  $\text{H}_2\text{O}_2$ , and the oxidants' effects on texture, chemistry surface, vanadium adsorption, and catalytic activity were characterized.

## 2. Experimental

### 2.1. Support and catalyst preparation

Cordierite monoliths (400 cpsi, 1 cm in diameter and 5 cm in length) were coated with a polymer blend by dip-coating as described elsewhere [12]. Briefly, the monoliths were coated with a polymeric blend of furan resin and polyethylene glycol (2:1), carbonized at 700 °C and later activated with  $\text{CO}_2$  at 900 °C for 4 h to develop further surface area and porosity. The as-prepared carbon-coated monoliths were treated with concentrated  $\text{HNO}_3$ ,  $\text{HNO}_3$  (2N),  $\text{H}_2\text{SO}_4$  (2N) or  $\text{H}_2\text{O}_2$ . All liquid oxidation treatments were carried out for 24 h at room temperature. Subsequently, the monoliths were thoroughly rinsed with distilled water. The oxidized carbon-coated monoliths were loaded with vanadium by means of an ion-exchange method with a solution of  $\text{NH}_4\text{VO}_3$  (and ca. 5 mg oxalic acid in 100 ml of solution) until equilibrium was reached. Under these conditions, the solution pH remains neutral, holding a yellow colour indicative of the presence of  $\text{VO}^{2+}$  species. Afterward, the monoliths were rinsed with distilled water, dried, and thermally treated in  $\text{N}_2$  at 350 °C.

### 2.2. Carbon support and catalyst characterization

The texture of the carbon-coated monolith supports was characterized by  $\text{N}_2$  physisorption, and surface chemistry was examined by temperature programmed desorption (TPD). The catalysts were characterized by means of  $\text{N}_2$  physisorption and XPS.

$\text{N}_2$  adsorption was performed on a Micrometrics ASAP 2020 at −196 °C. From the physisorption measurements with  $\text{N}_2$ , the specific surface area was calculated by applying the BET equation. The t-plot method was applied to calculate the micropore, and the BJH method was used to calculate the parameters related to mesoporosity. TPD measurements were carried out in a Micrometrics instruments. Samples were treated at 150 °C with a 30 ml/min stream of He to release all physically adsorbed complexes. After that, a temperature ramp of 10 °C/min from 150 to 1050 °C was applied. The  $\text{CO}_2$  and

$\text{CO}$  evolved during the runs were detected by a GC equipped with a TCD detector. Carbon materials show composite  $\text{CO}$  and  $\text{CO}_2$  signals that were deconvoluted and attributed to specific surface groups following some trends summarized in [13–15]. Finally, XPS for the internal plates of the monoliths were acquired with a Physical Electronic 5700 spectrometer equipped with a hemispherical electron analyser and Mg  $\text{K}\alpha$  X-ray exciting source (1253.6 eV, 15 kV, 300 W). It has been used as an internal standard for calibration  $\text{C}_{1s}$  (284.8 eV) considering a deviation  $\pm 0.2$  eV. Peak deconvolution shows the contribution of more than one species and their relative populations. In all cases the signal was adjusted to a mathematical response consistent with a Gaussian–Lorentzian distribution (80–20%, respectively) with a minimal  $\chi^2$  deviation.

### 2.3. Catalytic test

The catalytic tests were performed in a 14 mm i.d. quartz reactor. The gas (1000 ppmv NO, 1000 ppm  $\text{NH}_3$  and 10%  $\text{O}_2$  and Ar to balance) was forced to flow through the monolith channels. The gas spatial velocity per hour (GSVH) of the performance was around 34,000  $\text{h}^{-1}$  related to the carbon weight. The reaction temperature was set at 150, 250, and 350 °C and the reaction was allowed to proceed for 2 h to reach a steady state. A mass spectrometer (Balzers), which had previously been calibrated with cylinders of certified known composition, was used to analyze the gas stream. The NO conversion efficiency was calculated as follows:

$$\% \text{NO reduction} = \frac{(C_{\text{NO}}^i - C_{\text{NO}})}{C_{\text{NO}}^i} \times 100 \quad (1)$$

where  $C_{\text{NO}}^i$  is the initial concentration of NO and  $C_{\text{NO}}$  corresponds to its concentration once a steady state is reached.

## 3. Results and discussion

### 3.1. Textural characterization of activated and oxidized supports

Surface area and the pore volume distribution of the activated and subsequently oxidized supports are summarized in Table 1. The four oxidized carbon supports have similar pore size distribution and pore volume data (Table 1) than the activated carbon support. Moreover, adsorption–desorption isotherms also present a similar shape (not shown here). Hence, these both observations indicate that surface modification of the carbon supports has been successfully achieved without disrupting the original textural structures of activated coated monoliths and as explained above creating a high amount of oxygen surface groups [17]. Despite these similarities, there are some oxidation treatments that are more severe. Notably,  $\text{H}_2\text{O}_2$  and  $\text{H}_2\text{SO}_4$  oxidation treatment do not significantly change surface area ( $S_{\text{BET}}$ ), while concentrated  $\text{HNO}_3$  and 2N  $\text{HNO}_3$  oxidation treatments produce a much lower surface area. Based on these results, it can be concluded that textural properties

Table 1

Volume of pores and BET area of oxidized carbon-coated monoliths and 3 wt.% V of carbon doped catalysts

	$V_{\text{micro total}}$ (cc/g)	$V_{\text{micro}} (<0.7 \text{ nm})$ (cc/g)	$V_{\text{micro medium}}$ (cc/g)	$V_{\text{mesopore}}$ (cc/g)	$S_{\text{BET}}$ (m <sup>2</sup> /g)	Average $d_p$ (Å)
Activated support	0.017	0.012	0.005	0.033	653	–
HNO <sub>3</sub> (2N)	0.019	0.015	0.004	0.030	440	63
HNO <sub>3</sub> (c)	0.018	0.016	0.002	0.027	464	69
H <sub>2</sub> SO <sub>4</sub>	0.022	0.011	0.011	0.031	651	57
H <sub>2</sub> O <sub>2</sub>	0.011	0.008	0.003	0.031	616	65
3%V–HNO <sub>3</sub> (c)	0.009	0.006	0.003	0.028	274	63
3%V–HNO <sub>3</sub> (2N)	0.020	0.015	0.005	0.028	407	68
3%V–H <sub>2</sub> O <sub>2</sub>	0.017	0.013	0.004	0.028	609	66
3%V–H <sub>2</sub> SO <sub>4</sub>	0.014	0.010	0.004	0.027	458	68

depend on the oxidizing agent and oxidation treatment conditions [18,19] and that these oxidation treatment conditions can increase or decrease the surface area. As shown in Table 1, some other modifications occur in the pore distribution as a result of the oxidation treatments. The most remarkable change occurs on the H<sub>2</sub>O<sub>2</sub>-treated sample, where a certain degree of microporosity plugging occurs upon oxidation. In contrast, the samples treated with inorganic acids show a small increase in the microporosity. Later treatments may lead to some widening of the narrow micropores developed after CO<sub>2</sub> activation, resulting in increased accessibility for N<sub>2</sub> adsorption at –196 °C.

A decrease in surface area due to the mass increase associated with creation of new surface oxygen complexes was expected when HNO<sub>3</sub> was used as the oxidizing agent. However, some authors argue [20,21] that not only the amount of matter incorporated into the samples, but also other factors connected with the method of preparation (such as the

concentration of the HNO<sub>3</sub> solution) and the contact conditions may influence the textural properties of samples. Increased severity of the oxidation treatment due to higher concentrations of HNO<sub>3</sub> greatly decreases the surface area mainly due to a decrease in mesoporosity. Variation in microporosity is of little significance. This could also be explained by the stronger erosion caused by concentrated HNO<sub>3</sub> treatment widening the pores [22].

### 3.2. Chemical characterization of the activated and oxidized supports (TPD and XPS)

The chemical nature of the oxygen surface complexes fixed onto carbon-coated supports after the oxidizing treatments was studied by both XPS and TPD. TPD gives information about the composition of the most important oxygen groups present in the bulk while XPS gives information about the composition of the most external surface. Fig. 1 shows the CO and CO<sub>2</sub> TPD

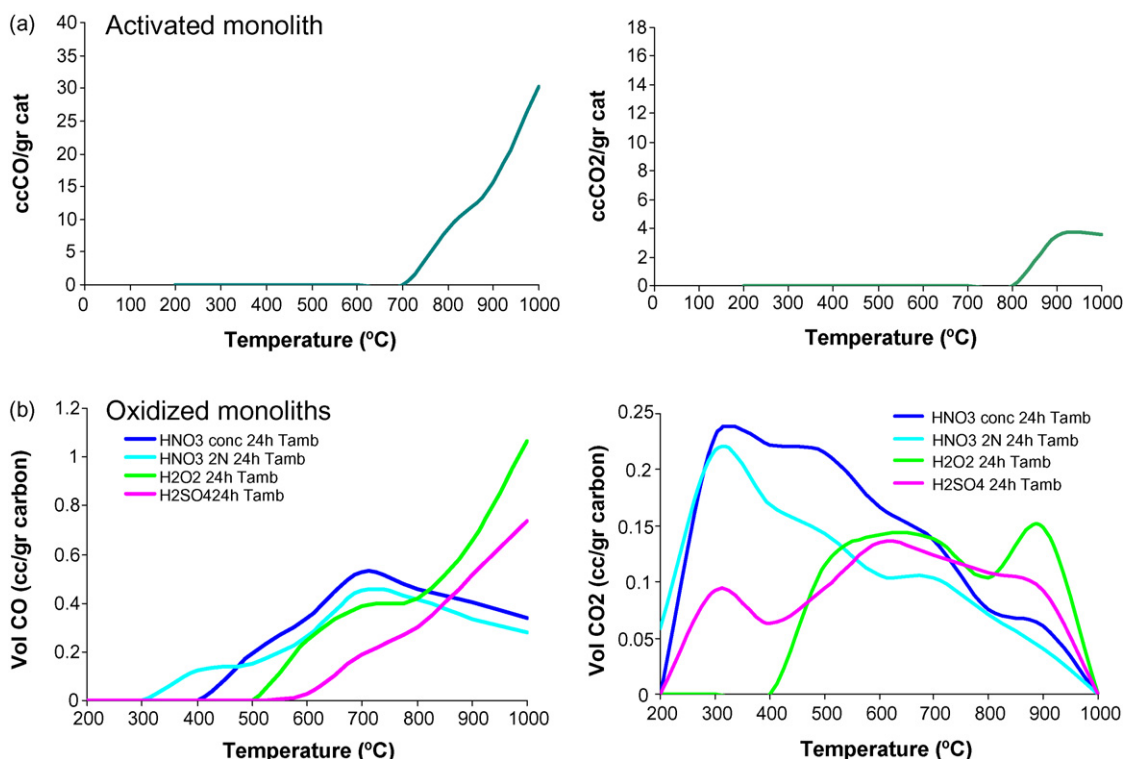


Fig. 1. TPD profiles of: (a) activated and (b) oxidized carbon-coated supports.

profiles for the four oxidized samples and the activated support. According to the literature [23,24,16], CO<sub>2</sub> peaks correspond mainly to acid groups, such as carboxylic groups (100–400 °C) and anhydride and lactone groups (600 °C). On the other hand, CO desorption may originate from the evolution of different types of oxygen surface groups such as phenol (650 °C), ether (700 °C), carbonyl (800 °C), quinone (850 °C), and pyrone (900 °C). As observed in Fig. 1, all oxidation treatments create a high amount of CO- and CO<sub>2</sub>-evolving groups, indicating that the oxidation treatments have successfully reached their goal: creation of a high number of oxygen surface groups without significantly changing the textural structure of the samples. Depending on the oxidizing agent and concentration, there are some notable differences worth commenting upon. Regarding the CO<sub>2</sub> profile deconvolution, it is observed that inorganic acids favoured the creation of oxygen surface groups that allow desorption at lower temperatures (from 200 to 700 °C), while oxidation with H<sub>2</sub>O<sub>2</sub> induces creation of oxygen surface groups which allow desorption at higher temperatures. More specifically, both HNO<sub>3</sub> treatments present a peak at low temperatures, which suggests the presence of a high number of carboxylic acid groups. H<sub>2</sub>SO<sub>4</sub> favours the desorption of groups evolved at higher temperatures, which can tentatively be attributed to lactones. H<sub>2</sub>O<sub>2</sub>, unlike the other oxidation treatments, does not promote the formation of low-temperature CO<sub>2</sub>-evolving groups. For CO evolution, the results in Fig. 1 indicate that carboxyl, ether, and phenol groups are most developed after HNO<sub>3</sub> treatments. The groups developed by H<sub>2</sub>O<sub>2</sub> treatment are mainly ascribed to carbonyl, quinone and pyrone. H<sub>2</sub>SO<sub>4</sub> oxidation seems to favour the creation of high temperature CO-evolving groups as well. These results are consistent with other authors [16] who found an increase in carboxylic acid groups after nitric acid treatment. The total amounts of CO and CO<sub>2</sub> evolved in TPD runs are shown in Table 2. The results indicate that H<sub>2</sub>O<sub>2</sub> oxidation fixes the lowest amount of CO<sub>2</sub>-evolving surface complexes, whereas HNO<sub>3</sub> oxidation treatments, both concentrated and 2N, fix the largest amount of these groups. Therefore, the CO/CO<sub>2</sub> ratio increases in the order HNO<sub>3</sub> (c) < HNO<sub>3</sub> (2N) < H<sub>2</sub>SO<sub>4</sub> < H<sub>2</sub>O<sub>2</sub>, indicating that the HNO<sub>3</sub> treatment creates the most acidic surface. Regardless of the oxidizing agent used, a general increase of surface acidity is observed. After any oxidation treatment, the CO/CO<sub>2</sub> ratio is between 1.7- and 3.6-fold lower than the non-oxidized samples, indicating the increased acidity of oxidized surfaces.

The binding energies (BE) and relative signal percentage of fitted C<sub>1s</sub>, O<sub>1s</sub> and V<sub>3p</sub> components were monitored. C<sub>1s</sub> and V<sub>3p</sub> data of the vanadium-containing carbon materials treated

Table 2  
TPD results of oxidized carbon-coated monoliths and activated monolith

	CO (cc/g)	CO <sub>2</sub> (cc/g)	CO + CO <sub>2</sub> (cc/g)	CO/CO <sub>2</sub>
Activated monolith	3.3	0.4	3.7	7.36
HNO <sub>3</sub> (c)	111.5	55.6	167.1	2.04
HNO <sub>3</sub> 2N	99.4	45.6	145.0	2.22
H <sub>2</sub> SO <sub>4</sub>	87.1	35.6	122.7	2.49
H <sub>2</sub> O <sub>2</sub>	136.9	32.5	169.4	4.29

Table 3  
XPS data

3 wt.% V carbon	HNO <sub>3</sub> (c)	HNO <sub>3</sub> (2N)	H <sub>2</sub> O <sub>2</sub>	H <sub>2</sub> SO <sub>4</sub>
BE (eV)	284.7 (60) 286.4 (28) – 289.6 (12)	284.7 (71) 286.4 (19) – 289.3 (10)	284.7 (70) 286.5 (17) – 289.4 (13)	284.6 (69) 286.3 (14) 288.8 (17) –

BE (eV) values and relative C<sub>1s</sub> peak percentage for vanadium-doped catalysts.

Table 4  
XPS data

3 wt.% V carbon	BE (eV)	V <sup>(+4)</sup> /V <sup>(+5)</sup>
HNO <sub>3</sub> (c)	–	Non-detected
HNO <sub>3</sub> (2N)	515.9 517.4	3.42
H <sub>2</sub> O <sub>2</sub>	515.9 517.8	0.64
H <sub>2</sub> SO <sub>4</sub>	515.5 517.0	0.16

V<sub>3p</sub> BE (eV) values and V<sup>4+</sup>/V<sup>5+</sup> ratio for vanadium catalysts.

with different wet chemical treatments are shown in Table 3 and Table 4. All oxidizing treatments increase the overall concentration of surface oxides, as evidenced by the increase of O<sub>1s</sub> (data not shown). In some treatments there is also a visible broadening of the C<sub>1s</sub> signal enveloped to higher BE indicative of the highly oxidized carbon species. With H<sub>2</sub>O<sub>2</sub> treatment, the contribution associated with carbonyl groups is negligible; the carboxylic groups (289.4 eV) represent 13% of the overall contribution and the peak localized at 284.4 eV might be related to non-functionalized carbon support. When HNO<sub>3</sub> (2N) was used for oxidation, the material exhibits an easily observable modification in the surface distribution. The BE at 286.4 eV, associated with the presence of phenolic–ether species, increases slightly, while the carboxyl species actually decreases. More significant changes are seen for treatment with concentrated HNO<sub>3</sub>. The contribution of C<sub>1s</sub> related to the non-functionalized support (284.7 eV) varies up to 60% and the phenolic–ether species increases to 28% of the signal. Finally, the H<sub>2</sub>SO<sub>4</sub> oxidation treatment apparently favoured the presence of less-oxidized species as carbonyl groups.

The observed differences between TPD and XPS data could be due to the differences between both techniques. Based on this interpretation, we consider that the TPD results agree well with those found in the literature, and that they allow for the quality of the whole sample. On the other hand, XPS results are limited to the surface, and these measurements have been performed in just one point. As a result, we expect their error to be higher.

### 3.3. Textural characterization of catalysts

Textural characterization of the catalysts was carried out by means of N<sub>2</sub> adsorption (Table 1). A decrease in the SSA values is measured for the catalysts in comparison with the supports.



This decrease has been previously reported by other authors [27–29] and was attributed to fixation of the active phase at the pore entrance. A main consequence of oxidation treatments is a higher or lower level of reduction in textural properties depending on the nature and concentration of the oxidation agent. Oxygen surface groups may be responsible for chemically controlled vanadium anchoring on the surface of the carbon supports. In particular, those groups with a strong acidic character (i.e. of carboxylic groups) might enhance the anchoring of vanadium, thereby resulting in a higher decrease of textural properties. As a result, the support exposed to concentrated  $\text{HNO}_3$  yields greater  $S_{\text{BET}}$  reduction while  $\text{H}_2\text{O}_2$  samples does not present a noticeable  $S_{\text{BET}}$  decrease.

### 3.4. Catalytic characterization and activity tests

Vanadium carbon-coated catalysts were tested in the SCR- $\text{NH}_3$  of NO at 150, 250, and 350 °C. For the sake of comparison, NO conversion from these runs was calculated assuming a first order rate equation with respect to NO and zero order with respect to  $\text{NH}_3$ :  $r_{\text{NO}} = k [\text{NO}]$  (1). In a previous work [29], it was found that the reaction is free of diffusional limitations. Fig. 2 shows the effect of oxidation conditions on catalytic activity for the vanadium-based catalysts. The selectivity towards  $\text{N}_2$  ranges from 80 to 90% in all the runs. Selectivity was calculated by following the  $\text{N}_2$ ,  $\text{N}_2\text{O}$  and  $\text{NO}_2$  concentration on-line in the mass spectrometer.

The presence of vanadium on the catalysts was evident based on the  $\text{V}_{3p}$  core level signal registered in the XPS spectra. Deconvolution of the  $\text{V}_{3p}$  region revealed two bands. The difference in BE between the signals was 1.5–1.9 eV, which matched the reported value for  $\text{V}_{3p}$ . This deviation might be indicative of an interaction between vanadium and the functionalized surface. Calculating the relative percentages,  $\text{V}^{(4+)}$  (515.5–515.9 eV) is the most abundant species if the material was previously treated with  $\text{HNO}_3$  (2N). The relative atomic ratios,  $\text{V}^{4+}/\text{V}^{5+}$ , are inverted for the rest of the liquid oxidation treatments. It is clear that the extension of functionalization governs the vanadium spreading, but the

nature of the carbon surface determines binding onto surface functional groups.

As evaluated and according to the results shown in Fig. 2 and noted by other authors [5,6], the amount of adsorbed vanadium, its dispersion, and the oxidation state of the active element is strongly dependent on the surface chemistry and porosity of carbon supports. In this sense, catalytic activity seems to have a close relationship to the amount and type of oxygen surface groups created by oxidative treatments. In addition, the amount of vanadium  $\text{V}^{4+}$  adsorbed ( $\text{V}^{4+}/\text{V}^{5+}$ ) by each support appears to be a factor. The support properties and catalyst activity showed a well-fitted correlation between the number of acidic groups and the efficiency of NO reduction. Samples oxidized with  $\text{HNO}_3$  show the highest number of carboxylic groups and exhibit the highest NO conversion. According to the literature [5,6,30–32], acidic groups may promote dispersion of the metallic phase onto the carbon surface. This fact may be the source of the higher NO conversion shown by the sample oxidized with  $\text{HNO}_3$  (2N). Although the sample treated with concentrated  $\text{HNO}_3$  exhibits an even higher number of carboxylic surface groups, the number of non-accessible vanadium sites limit its activity. The extremely strong acidic surface character of the sample treated with concentrated nitric acid seems to be responsible for an excessively strong adsorption of  $\text{NH}_3$  that prevents its desorption during reaction, resulting in reduced activity.

Although oxidation with inorganic acids leads to a poorly developed pore structure, it creates a higher number of acidic groups, which, in turn, enhance the adsorption of vanadium. Consequently, the catalytic activity of these samples remains higher than those oxidized with  $\text{H}_2\text{O}_2$ . This result highlights the fact that although proper development of the porous structure is fundamental for avoiding pore blockage, the presence of oxygen surface functionalities is quite important for achieving an adequate distribution and fixation of the active phase. Moreover, the presence of these groups may also contribute to the adsorption of the reactants during NO reduction [25,26].

## 4. Conclusions

This work has shown the influence of acid treatments of the carbon support on the reduction of NO with 3 wt.% vanadium-loaded carbon-coated monoliths. For a series of four samples, NO reduction activity follows the trend of  $\text{HNO}_3$  (2N) >  $\text{HNO}_3$  (c) >  $\text{H}_2\text{SO}_4$  >  $\text{H}_2\text{O}_2$ . This result coincides with the middle values of  $\text{CO}_2$  evolved during TPD and the middle areas of  $\text{O}_{1s}$  obtained by XPS runs. This result also highlights that the effects of the acid treatments are closely related to the oxygen surface groups density created by the oxidation processes.  $\text{HNO}_3$  treatment produces the highest number of active surface complexes as carboxyls and lactones, which enhances vanadium dispersion and catalytic activity.  $\text{H}_2\text{SO}_4$  treatment, however, produces more stable oxygen surface groups such as carbonyls and phenols that do not further promote NO reduction.  $\text{H}_2\text{O}_2$  treatment produces the most stable oxygen surface groups, as ether or pyronic groups that can actually reduce catalyst activity.

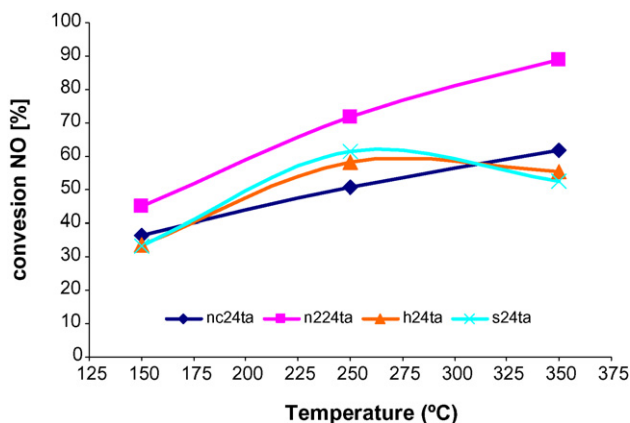


Fig. 2. NO conversion achieved for four catalysts oxidized with  $\text{HNO}_3$  (c),  $\text{HNO}_3$  (2N),  $\text{H}_2\text{SO}_4$  (2N) and  $\text{H}_2\text{O}_2$ . All catalyst supports are doped with 3 wt.% vanadium.

The acidic character of the surface is of key importance for achieving a high NO reduction efficiency. Concentrated HNO<sub>3</sub> treatment yields the highest surface acidity, but it seems to favour NH<sub>3</sub> adsorption, thereby reducing catalytic activity. Finally, the high number of surface oxygen complexes produced affects the pore structure of the supports but its influence on the catalytic activity is much weaker than the effect of surface chemistry.

### Acknowledgments

The authors wish to thank the Spanish MMA for financial support (Project MMA437/2006/3-13.1) and the EU for project EUROCAT 63011. A. Boyano is indebted to CSIC for her predoctoral grant.

### References

- [1] J. Benitez (Ed.), *Process Engineering and Design for Air Pollution Control*, 254, Prentice-Hall, Englewood Cliffs, NJ, 1993 (Chapter 6).
- [2] G. Busca, L. Lietti, I. Nova, P. Forzatti, A. Baiker, *Appl. Catal. B: Environ.* 19 (1998) 1–36.
- [3] A. Boyano, M.E. Gálvez, M.J. Lázaro, R. Moliner, *Carbon* 44 (2006) 2399–2403.
- [4] Z. Huang, Z. Zhepping, Z. Liu, *Appl. Catal. B: Environ.* 39 (2002) 361–368.
- [5] G. Marban, R. Antuña, A.B. Fuertes, *Appl. Catal. B: Environ.* 41 (2003) 323–338.
- [6] E. García-Bordejé, M.J. Lázaro, R. Moliner, P.M. Álvarez, V. Gómez-Serrano, J.L.G. Fierro, *Carbon* 44 (2006) 407–417.
- [7] B.R. Puri (Ed.), *Chemistry and Physics of Carbon*, Marcel Dekker, New York, 1970, p. 191.
- [8] F. Rodríguez-Reinoso, J. Garrido, J.M. Martín-Martínez, M. Molina-Sabio, R. Torregorsá, *Carbon* 27 (1989) 23.
- [9] B. Prandhan, N.K. Sandle, *Carbon* 37 (1999) 1323–1332.
- [10] R.C. Bansal, J.B. Donner, F. Stoeckli, *Active Carbon*, Marcel Dekker, New York, p. 198.
- [11] K. Forger, *Catalysis (Science and Technology)*, Springer Verlag, Heidelberg, 1984, p. 227.
- [12] E. García-Bordejé, L. Calvillo, M.J. Lázaro, R. Moliner, *Appl. Catal. B: Environ.* 50 (2004) 235–242.
- [13] J.L. Falconer, J.A. Schwarz, *Catal. Rev.-Sci. Eng.* 25 (1983) 141.
- [14] H.P. Boehm, G. Bewer, in: *Proceeding of the 4th London Carbon and Graphite Conference*, London, UK 1974, p. 344.
- [15] H.P. Boehm, *Carbon* 32 (1994) 759–769.
- [16] J.L. Figueiredo, M.F.R. Pereira, M.M.A. Freitas, J.J.M. Orfao, *Carbon* 37 (1999) 1379–1389.
- [17] P.A. Bazula, A.H. Lu, J.J. Nitz, F. Schüth, *Microporous Mesoporous Mater.* 108 (2008) 266–275.
- [18] M. Domingo-García, F.J. Lopez-Garzon, M. Perez-Mendoza, *J. Colloid Inter. Sci.* 40 (2000) 222–233.
- [19] A. Gil, G. de la Puente, P. Grange, *Microporous Mater.* 61 (1997) 12–51.
- [20] V. Gómez-Serrano, M. Acedo-Ramos, A.J. López-Peinado, C. Valenzuela-Calahorra, *Thermochim. Acta* 291 (1997) 109–115.
- [21] R.C. West (Ed.), *Handbook of Chemistry and Physics*, 59th ed., CRC Press, Boca Raton, FL, 1987.
- [22] C. Moreno-Castilla, M. Ferro-García, J. Joly, I. Bautista-Toledo, I. Carrasco-Marín, J. Rivera-Utrilla, *Langmuir* 11 (1995) 4386–4392.
- [23] A. Quintanilla, J.A. Casas, J.J. Rodríguez, *Appl. Catal. B: Environ.* 76 (2007) 135–145.
- [24] G.S. Szymanski, Z. Karpinski, S. Biniak, A. Swiatkowski, *Carbon* 40 (2002) 2627–2639.
- [25] M.D. Amiridis, R.V. Duevel, I.E. Wachs, *Appl. Catal. B: Environ.* 20 (1999) 111–122.
- [26] J.S. Noh, J.Á. Schwarz, *Carbon* 28 (1990) 675–682.
- [27] Z. Zhu, L.R. Radovix, G.Q. Lu, *Carbon* 38 (2000) 451–464.
- [28] M.J. Lázaro, A. Boyano, M.E. Gálvez, M.T. Izquierdo, R. Moliner, *Catal. Today* 119 (2007) 175–180.
- [29] E. García-Bordejé, M.J. Lázaro, R. Moliner, J.F. Galindo, J. Sostres, A.M. Baro, *Appl. Catal.* 228 (2004) 135–142.
- [30] Z. Zhu, Z. Liu, S. Iiu, H. Niu, *Appl. Catal. B: Environ.* 30 (2001) 267–276.
- [31] A. Martín-Gullón, C. Prado-Bugüete, F. Rodríguez-Reinoso, *Carbon* 31 (1993) 1009.
- [32] M.C. Roman-Martínez, D. Cazorla-Amoros, A. Linares-Solano, C. Salinas-Martínez de Lecea, H. Yamashita, M. Anpo, *Carbon* 33 (1968) 161.